ChemComm

Accepted Manuscript

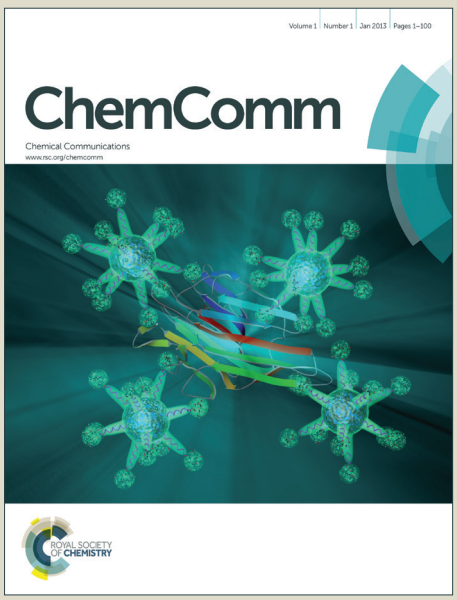

ROYAL SOCIETY OF CHEMISTRY

www.rsc.org/chemcomm

Chemical Communications RSCPublishing

COMMUNICATION

Topotactic elimination of water across a C-C ligand bond in a dense 3-D metal-organic framework†

Cite this: DOI: 10.1039/x0xx00000x

Hamish H.-M. Yeung,[a,b] Monica Kosa,[c] John M. Griffin,[d] Clare P. Grey,[d] Dan T. Major[c] and Anthony K. Cheetham*[a]

Received xxth xxx 2014,
Accepted xxth xxx 2014

DOI: 10.1039/x0xx00000x

www.rsc.org/

Upon heating, lithium L-malate undergoes topotactic dehydration to form a phase containing the unsaturated fumarate ligand, in which the original 3-D framework remains intact. Insight into this unusual transformation has been obtained by single crystal X-ray diffraction, MAS-NMR, *in-situ* powder X-ray diffraction and DFT calculations.

In recent years, metal-organic frameworks (MOFs) have opened up new avenues in the search for novel functional materials, owing to their wide compositional scope, modular structure and facile synthesis.[1–3] Coordination bonding between metal ions and bridging organic ligands gives rise to extended 1-, 2- and 3-dimensional structures, with diverse properties, including gas sorption,[4] magnetism,[5] chirality[6] and multiferroicity,[7] arising from the synergy between the constituent organic and inorganic units. MOFs have also been used as templates for post-synthetic functionalization[8] and topochemical reactions,[9–11] in which the orientations of the organic molecules in the precursor crystal direct the structure of the product.[12,13] The crystal engineering approach to topochemical reactions has traditionally been dominated by non-covalent forces, which can accommodate the crystal strain accompanying bond breaking and formation.[14] Despite their relative rigidity, however, coordination bonds impart extra stability to organic molecules, allowing access to more demanding conditions, such as higher temperatures and pressures, as well as giving excellent control over molecular conformations.[15]

We describe herein the first example of a topochemical elimination reaction within a non-porous MOF, which occurs spontaneously in a single crystal-to-single crystal manner despite a lack of accessible porosity in the conventional sense. The crystal structure and thermogravimetry of lithium L-malate [Li_2(L-$C_4H_4O_5$)], **1**, was described in a previous article, in which we reported that the relative flexibility of Li-O bonds, compared to stronger transition metal-oxygen bonds, allows MOF frameworks to distort enough to accommodate ligand solution solutions.[16] **1** undergoes a two-step mass loss on heating, whereby decomposition of the main framework at 400 °C is preceded by a loss of approx. 12 wt. %, which corresponds to the combined mass of one proton and one hydroxyl group per malate ligand. Upon closer investigation, it was observed that large single crystals remained intact after various heat treatments between 280-350 °C, allowing the crystal structure of the resulting mixed-ligand MOF, [Li_2(L-$C_4H_4O_5$)$_{1-x}$($C_4H_2O_4$)$_x$], **2(*x*)**, to be determined by single crystal X-ray diffraction for various values of *x* (see Table S1 in the Supplementary Information).

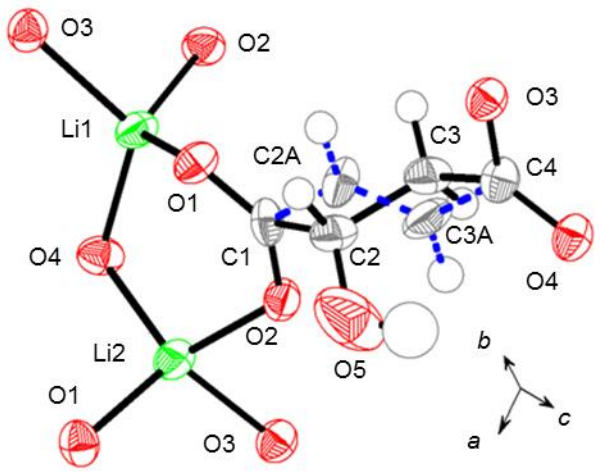

Figure 1. Ortep extended asymmetric unit of **2(0.77)** determined by single crystal X-ray diffraction, showing the original L-malate atoms joined by black lines and the unsaturated fumarate ligand (dashed blue lines). ADP ellipsoids are shown at 50 % (20 % for H).

The crystal structure of **2(*x*)** consists of a 3-D framework of LiO_4 tetrahedra bridged by dicarboxylate L-malate and fumarate ligands, which reside in the same crystallographic location with fractional occupancies of (1-*x*) and *x*, respectively (Fig. 1). The *trans*- configuration of the fumarate ligand suggests that water has been eliminated from across the L-malate C-C bond in a stereospecific manner directed by its fixed conformation within the 3-D MOF (Scheme 1). All compositions of **2(*x*)** analysed

were found to be isostructural with **1** in space group *R*3, indicating that framework chirality is preserved even when 80 % of ligands present are achiral.

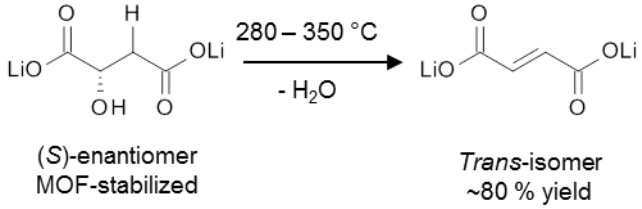

Scheme 1. Stereospecificity of the topotactic dehydration of Li_2(L-malate) directed by its conformation in the MOF.

Whilst the parent compound **1** exhibits disorder between two crystallographic positions of the L-malate hydroxyl group,[16] the structure determinations of **2(*x*)** only found significant electron density in one position, O5. This suggests a preference for dehydration of the minor site over the major site, which may arise from local differences in stability owing to hydrogen bonding. Further evidence was obtained from MAS-NMR spectra of **2(*x*)**, which revealed small but significant changes in chemical shifts upon partial dehydration (See S2, Fig. S1 and Table S2). ^{1}H and ^{13}C NMR spectra of **2(0.77)** in D_2O, and FTIR spectra of **2(*x*)** at different stages of dehydration are consistent with the above observations (See Figs. S2-4).

The relative formation enthalpies of **2(*x*)** at various compositions were calculated at 0 K using Density Functional Theory (DFT) within the PBE functional approximation,[17] alone and with dispersion corrections D2[18] and D3[19] (Table S3). Enthalpies were also calculated including Zero-Point Energy and vibrational contributions at 300 K, showing similar trends and so will not be discussed here. The dehydration reaction was shown to be endothermic, as expected for elimination of water to form a C=C bond. At the PBE+D3 level of theory, the complete dehydration reaction requires 81.8 kJ mol^{-1} and extrapolation of the data to x = 0 reveals that this includes 13.7(3) kJ mol^{-1} needed to break the strong hydrogen bonding between hydroxyl groups before the first water is lost (Fig. S5). The unfavourable enthalpy is primarily offset, of course, by the entropy of the water vapour at the decomposition temperature. On the basis of a value for the entropy of water of 188.8 J mol^{-1} K^{-1},[20] decomposition would be expected at 160 °C, in good agreement with our observations.

The structural evolution of **2(*x*)** with increasing temperature was studied using *in-situ* variable-temperature (VT) powder X-ray diffraction. Non-linear shifts in the positions of the Bragg peaks were observed and Le Bail refinement of the unit cell parameters revealed three distinct processes: i) expansion of the unit cell of **1**, ii) dehydration to form **2(*x*)**, and iii) expansion of the unit cell of the dehydrated MOF alongside decomposition to form Li_2CO_3 (Fig. 3 and S6-10). Whilst the variations in unit cell parameters are highly anisotropic, the average volumetric thermal expansion of each process is relatively constant (α_V = 97(8) × 10^{-6} K^{-1}, 115(18) × 10^{-6} K^{-1} and 103(9) × 10^{-6} K^{-1}, for i-iii, respectively). It should be noted that the transition temperatures were lower than observed in single crystal studies, partly due to kinetic effects of powder particle size reduction.

From 30 °C to 150 °C (process i), thermal expansion of **1** occurs predominantly in the crystallographically equivalent *a*- and *b*- directions, with negligible change in *c*. The mechanical properties of **1**, as reported previously,[16] depend strongly on the hydrogen bonded trimer of hydroxyl groups, which causes contraction in the *ab*-plane. At raised temperatures, however, they may be more easily broken by thermal vibrations than the stronger covalent bonds which connect the MOF along the *c*-axis. Hence the coefficients of thermal expansion in the two orthogonal directions, α_a and α_c, are 49.0(1.5) × 10^{-6} K^{-1} and -1(11) × 10^{-6} K^{-1}, respectively.

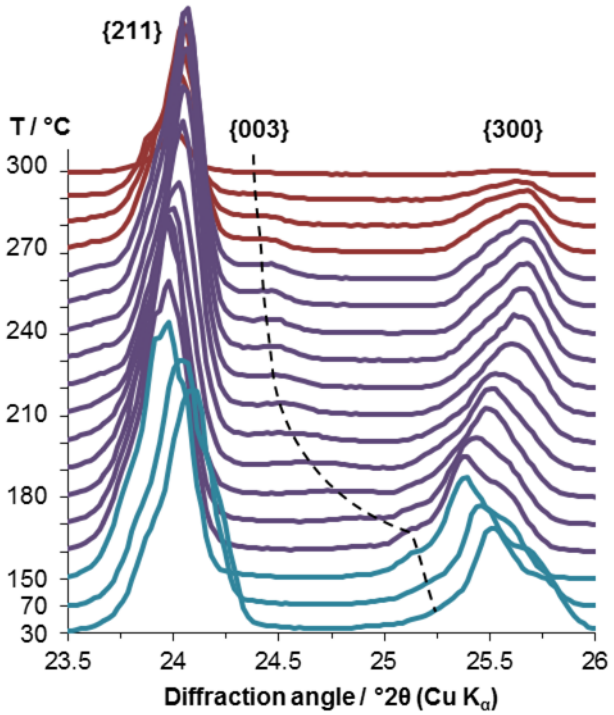

Figure 3. VT-powder X-ray diffraction data for **2(*x*)** in *R*3, showing the expansion, topotactic dehydration and decomposition processes in blue, purple and red, respectively.

In the region 150 °C - 240 °C (process ii), the *c*-axis undergoes rapid expansion (α_c = 311(19) × 10^{-6} K^{-1}), whilst the *a*-axis contracts significantly (α_a = -98(7) × 10^{-6} K^{-1}). Although these values are one order of magnitude larger than common materials and similar to the colossal positive and negative thermal expansion observed in silver(I) hexacyanocobaltate(III)-type materials recently reported,[21] the behaviour in this system is irreversible owing to the accompanying dehydration process. The effect of hydrogen bonding has already been weakened below 150 °C, and so expansion along *c* must be due to the lengthening of the ligand and the increase in its rigidity (owing to π-conjugation).

Above 240 °C, the distinct change in α_a and α_c (24(2) × 10^{-6} K^{-1} and 55(8) × 10^{-6} K^{-1}, respectively), indicates that the main dehydration process is essentially complete. The resulting MOF undergoes anisotropic thermal expansion up until complete

decomposition to form Li_2CO_3, which precludes the formation of the fully dehydrated material, $Li_2(C_4H_2O_4)$, **2(1)**. From single crystal studies, we estimate that the maximum extent of dehydration in this system is in the region $0.8 \leq x_{max} \leq 1$.

Attempts to synthesize hypothetical **2(1)** directly from fumaric acid *via* both solution and solvothermal crystallization resulted in the discovery of a polymorphic phase in *P*-1, **3**, whose framework connectivity is very different to **2(1)** (I^1O^2 and I^3O^0, respectively, according to the notation of Cheetham *et al.*).[2] Notably, **2(1)** was not observed under any conditions employed, and so a detailed comparison of the two structures was undertaken (see S3 and Fig. S11-13). Several similarities in the structures of **2(1)** and **3** were found, but the average Li-O bond valence sum of **3** is 6 % lower than that of **2(1)** (1.02 and 1.08, respectively), suggesting that the ionic bonding in **2(1)** is stronger. In contrast, the X-ray density of **3** is 1.809 g cm^{-3}, 25 % greater than that of the hypothetical fully dehydrated phase, **2(1)**, suggesting that dispersion forces are stronger in **3**.

The relative enthalpies of **3** and **2(1)** were calculated using DFT methods at 0 K, revealing that, without dispersion corrections, **2(1)** is 9.6 kJ mol^{-1} more stable than **3**. However, when dispersion corrections are applied, the relative energies are reversed, such that **3** is more stable than **2(1)** by 12.44-13.20 kJ mol^{-1}, depending on the level of theory (see Table S4 for values) This confirms that dispersion forces related to the packing density dominate the synthetic landscape for the formation of $Li_2(C_4H_2O_4)$ in solution, rather than the ionic contributions from Li-O bonding, and that topotactic dehydration offers a unique route to the otherwise unobtainable phase **2** (Scheme 2). Furthermore, it emphasizes the importance of full consideration of non-covalent interactions in theoretical calculations involving hybrid systems such as MOFs, as observed previously.[22–24]

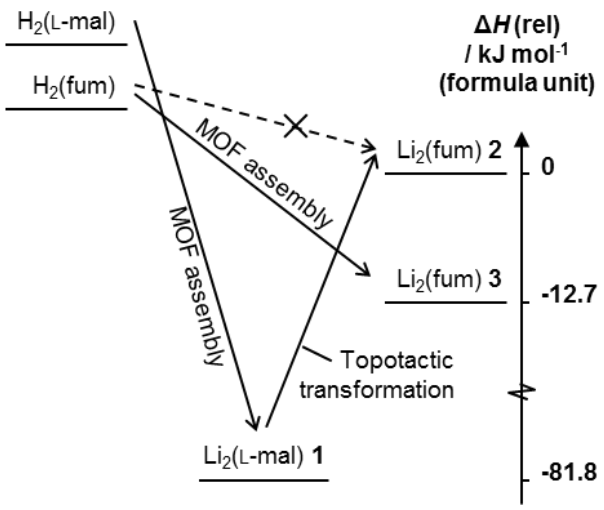

Scheme 2. Reaction routes from precursor ligands L-malic acid and fumaric acid (H_2(L-mal) and H_2(fum), respectively) to **1**-**3** *via* MOF assembly and topotactic transformation, and the calculated relative formation enthalpies of each phase at the PBE+D3 level of theory.

In summary, we have described the topotactic transformation of a dense 3-D MOF, **1**, in which the stereospecific elimination of water occurs across the ligand's central C-C bond to form a C=C double bond with a *trans*-configuration. Remarkably, despite the lack of conventional porosity, the water molecules produced can escape the framework leaving the ligand-lithium binding intact, and so the resulting framework retains the connectivity and crystallographic symmetry found in the starting material. Furthermore, the dehydration process results in colossal and irreversible positive and negative thermal expansion of the MOF framework. This is another striking example of the remarkable flexibility that is exhibited by many MOFs,[16,21,25] resulting in this case from the combination of chemical substitution and framework dynamics induced by thermal treatment. Our discovery reveals a new route to Post Synthetic Modification in dense MOFs, *via* the thermal dehydration of the ligand moiety. Phase **2** could potentially undergo further functionalization by addition to the C=C group, but unlike phase **3** is unobtainable *via* conventional means. The broad temperature and time-dependent nature of the thermal dehydration allow for good stoichiometry control in the resulting mixed-ligand MOF. On the other hand, our observations demonstrate that the additional stability imparted by MOF formation to organic molecules (L-malic acid decomposes completely to form gaseous products above 150 °C) allows simple and efficient thermal reactions in the solid state to be utilised that might otherwise require more complex reaction routes in solution. By stabilizing the molecule in a 3-D framework, the functionalization also occurs in a stereospecific manner, which demonstrates that such solid state reactions of MOFs could be usefully integrated into more mainstream organic synthesis methodology.

We thank Giulio Lampronti and Sebastian Henke for assistance with VT-XRD measurements and acknowledge the financial support of the EPSRC and ERC (Advanced Investigator Award, AKC). HHMY acknowledges support from the World Premier International Research Center Initiative on Materials Nanoarchitectonics (WPI-MANA) from MEXT, Japan.

Notes and references

[a] Department of Materials Science and Metallurgy, Cambridge University, Charles Babbage Road, Cambridge, UK, CB3 0FS.
[b] International Center for Young Scientists, WPI Center for Materials Nanoarchitectonics, National Institute of Materials Science, 1-1 Namiki, Tsukuba, Ibaraki, 305-0044, Japan.
[c] Department of Chemistry, Faculty of Exact Sciences and the Lise Meitner-Minerva Center of Computational Quantum Chemistry, Bar Ilan University, Ramat Gan, Israel, IL-52900.
[d] Department of Chemistry, Cambridge University, Lensfield Road, Cambridge, UK, CB2 1EW.
*Corresponding author, e-mail: akc30@cam.ac.uk.

† Electronic Supplementary Information (ESI) available: experimental procedures, crystallography, NMR, DFT, and XRD. Full crystallographic details are available in cif format from the CCDC, numbers 1018021-1018024. See DOI: 10.1039/c000000x/

1. S. Kitagawa, R. Kitaura, and S. Noro, *Angew. Chem., Int. Ed. Engl.*, 2004, **43**, 2334–75.

2. A. K. Cheetham, C. N. R. Rao, and R. K. Feller, *Chem. Commun.*, 2006, 4780–4795.

3. G. Férey, *Chem. Soc. Rev.*, 2008, **37**, 191–214.

4. X. Zhao, B. Xiao, A. J. Fletcher, K. M. Thomas, D. Bradshaw, and M. J. Rosseinsky, *Science*, 2004, **306**, 1012–5.

5. M. Kurmoo, *Chem. Soc. Rev.*, 2009, **38**, 1353–79.

6. D. Bradshaw, J. B. Claridge, E. J. Cussen, T. J. Prior, and M. J. Rosseinsky, *Acc. Chem. Res.*, 2005, **38**, 273–82.

7. P. Jain, V. Ramachandran, R. J. Clark, H. D. Zhou, B. H. Toby, N. S. Dalal, H. W. Kroto, and A. K. Cheetham, *J. Am. Chem. Soc.*, 2009, **131**, 13625–7.

8. S. M. Cohen, *Chem. Rev.*, 2012, **112**, 970–1000.

9. G. M. J. Schmidt, *Pure Appl. Chem.*, 1971, **27**.

10. W. L. Leong and J. J. Vittal, *Chem. Rev.*, 2011, **111**, 688–764.

11. G. K. Kole and J. J. Vittal, *Chem. Soc. Rev.*, 2013, **42**, 1755–75.

12. R. Medishetty, L. L. Koh, G. K. Kole, and J. J. Vittal, *Angew. Chem., Int. Ed. Engl.*, 2011, **50**, 10949–52.

13. M.-H. Xie, X.-L. Yang, and C.-D. Wu, *Chem. - Eur. J.*, 2011, **17**, 11424–7.

14. K. Biradha and R. Santra, *Chem. Soc. Rev.*, 2013, **42**, 950–67.

15. H. H.-M. Yeung and A. K. Cheetham, *Dalton Trans.*, 2014, **43**, 95–102.

16. H. H.-M. Yeung, W. Li, P. J. Saines, T. K. J. Köster, C. P. Grey, and A. K. Cheetham, *Angew. Chem., Int. Ed. Engl.*, 2013, **52**, 5544–7.

17. J. Perdew, K. Burke, and M. Ernzerhof, *Phys. Rev. Lett.*, 1996, **77**, 3865–3868.

18. S. Grimme, *J. Comput. Chem.*, 2006, **27**, 1787–1799.

19. S. Grimme, J. Antony, S. Ehrlich, and H. Krieg, *J. Chem. Phys.*, 2010, **132**, 154104.

20. J. D. Cox, D. D. Wagman, and V. A. Medvedev, *CODATA Key Values for Thermodynamics*, Hemisphere Publishing Co., New York, 1984.

21. A. L. Goodwin, M. Calleja, M. J. Conterio, M. T. Dove, J. S. O. Evans, D. A. Keen, L. Peters, and M. G. Tucker, *Science*, 2008, **319**, 794–797.

22. H. H.-M. Yeung, M. Kosa, M. Parrinello, P. M. Forster, and A. K. Cheetham, *Cryst. Growth Des.*, 2011, **11**, 221–230.

23. B. K. Chang, N. C. Bristowe, P. D. Bristowe, and A. K. Cheetham, *Phys. Chem. Chem. Phys.*, 2012, **14**, 7059–7064.

24. H. H.-M. Yeung, M. Kosa, M. Parrinello, and A. K. Cheetham, *Cryst. Growth Des.*, 2013, **13**, 3705–3715.

25. L. Sarkisov, R. L. Martin, M. Haranczyk, and B. Smit, *J. Am. Chem. Soc.*, 2014, **136**, 2228–31.

